Proceedings of the Sixth International Conference on
Railway Technology: Research, Development and Maintenance
Edited by: J. Pombo
Civil-Comp Conferences, Volume 7, Paper 6.4
Civil-Comp Press, Edinburgh, United Kingdom, 2024
ISSN: 2753-3239, doi: 10.4203/ccc.7.6.4

Minimization of Impact Forces on Crossings by Railhead Profile Optimization

G. Megna and A. Bracciali

**Department of Industrial Engineering of Florence (DIEF),
University of Florence
Italy**

Abstract

High vertical loads due to running over rail discontinuities, such as joints and turnouts, generate relevant mechanical vibrations, noise, and wear. This problem is also relevant for unworn crossings because they are not optimized to match the shape of the passing wheels. This study presents a new approach for the geometric railhead design of crossings installed in turnouts with tight curve radii, which are mainly travelled in the through direction, introducing the concept of conformal crossing for the most common wheel profile in Europe, S1002. Starting from the existing geometry of conventional crossings, a 3D model of a conformal crossing is developed, and sections are extrapolated to perform multibody simulations that include wheel-rail contact calculation with variable rail profiles. The results were then compared with those obtained for the conventional crossing. Results show that conformal crossing can prevent vertical dynamic loads in the through route. The resulting increase in the impact loads when running along the diverging route was mitigated by further simple and effective modifications of the crossing.

Keywords: crossing, wheel-rail interaction, railway vehicle dynamics, rail profile, contact force, wheel profile.

1 Introduction

Turnouts are composed of switches and crossings (S&C). While running on switches is relatively smooth, running over crossings often generates an unpredictable interaction, as multiple wheel-rail contact points can be found along the path. This is because of the highly variable geometry of the rail profile, resulting in relevant impacts and vertical forces. The nomenclature of the turnout and common crossing components is shown in Figure 1. Therefore, a progressive transition is a key element in reducing the dynamic forces between different profiles and the effects of rail discontinuities. This is common for switch and stock rails, and a similar concept has been applied to insulated rail joints [1].

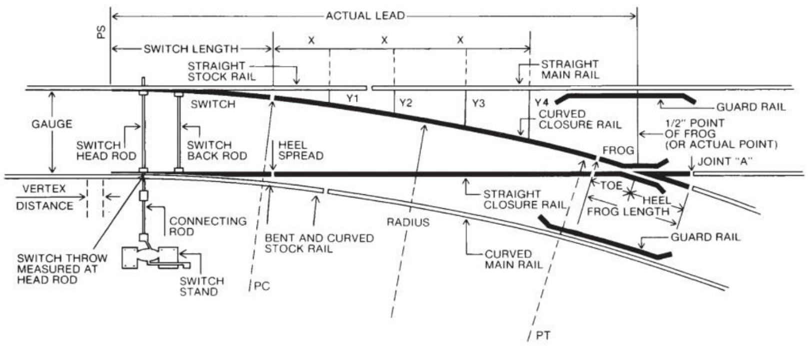

Figure 1: (Right-hand) turnout nomenclature.

1.1 General description of railway crossings

Unless crossings with a swing nose are used [2], the most important discontinuity in the crossing is located in the region in which the load is transferred from the wing rail to the nose. It can be described as a vertical dip-angle irregularity that can be modelled using a linear analytical approach [3]. An increase in the impact angle results in an increase in impact noise and impact loads. Therefore, there is a need for design and maintenance processes that are able to keep such an angle as small as possible [4]. Moreover, sharp radius (high tangent) turnouts exhibit larger crossing angles, resulting in greater damage [5].

The behaviour of a crossing over time is not easily predictable because the damaging processes depend on several factors. However, it worsens rapidly as the impact forces are present after the installation of the crossing. This is because the design of the crossing as a railhead profile is not optimized to match the shape of the passing wheels. Although the available standards [6] describes a number of elements devoted to the reduction of discontinuities (such as wing entry ramps and wheel ramps), high vertical load peaks cannot be avoided under all service conditions.

Multibody simulations on measured in-service crossings showed dip angles values up to 28 mrad and an almost linear correlation with the maximum wheel-rail contact force [7]. The dip angle irregularity can be correlated to the dynamic force with an analytical formulation [8], that at a travelling speed of 100 km/h returns a dynamic impact factor (DIF), defined as the ratio between dynamic and static loads, of about 3.9.

This paper describes the results of a study aimed at evaluating the effects of an asymmetric conformal profile of a crossing with a high crossing angle, primarily designed to reduce impact forces in the through route. The application of the complementary S1002 wheel profile to the crossing shape was first evaluated to obtain a theoretically perfect conformal contact while running over a crossing optimized for the through route. A large number of cross-sections extracted from a solid model of the crossing were implemented into a multibody model to evaluate the accuracy of the approach. The same process is repeated in the diverging route to observe whether the optimized shape increases the impact in that situation. Further optimization is then performed in the diverging route, reaching promising results, as speed restrictions do not appear to be needed in this condition.

The vehicle model used in the present analysis was the same as that used in the benchmark exercise [9], which shows numerous simulations of vehicles running in different scenarios, including the switch panel and crossing panel, both through and diverging routes. The results of the benchmark [10] confirmed the criticality of negotiating the crossing area.

For the crossing cases higher DIF values were observed for the 56E1V-R245-1:9.25 crossing compared to the 60E1-R760-1:15 crossing, although lower speeds were considered (100 km/h instead of 160 km/h). Simulations over the crossing panel were performed separately from those over the switch panel because the dynamic effects of the latter were considered negligible for the results over the crossing panel. This was confirmed by simulations that considered full turnout [11].

1.2 State of the art and existing solutions

Several attempts have been made to optimize the shape of the crossing nose according to the wheel profile. A numerical approach [12] has shown a beneficial effect in increasing the height and width of the crossing nose, whereas a reduction in the impact angle of approximately 10% was achieved with combined optimization for several measured wheel profiles of both the wing rail and crossing nose [13].

The reduction of the impact loads can also be pursued either by optimizing the stiffness of the track components, i.e., rail pads and under sleeper pads, [14] or by evaluating both the geometric shape and the support stiffness of the crossing [15]. For example, decreasing the crossing support stiffness from 500 MN/m to 85 MN/m reduced the vertical contact force by approximately 30%. The stiffness can be optimized along the crossing panel to minimize specific failure modes such as ballast settlement or wear and RCF [16]. A resiliently mounted nose concept was introduced and analyzed using multibody simulations [17]. However, these optimization processes led to an improved crossing shape and supporting stiffness, which mitigated, but did not prevent, high dynamic loads.

The main issue regarding large-angle crossing geometry lies in their symmetrical (*straight common crossing*) design, which makes no distinction between the through and diverging routes. Both the wing rail and nose geometries are the same in either direction, even if a large number of turnouts are rarely travelled in the diverging route. This is particularly true for large-angle crossings laid on a plain line, whose maximum speed on the diverging route is very low.

One of the most common turnouts installed on conventional lines in Italy is the 60E1-170-0.12 type, which can travel up to 200 km/h in the through direction and 30 km/h only in the diverging route (resulting in a 60 mm cant deficiency). These running conditions are completely different; thus, the perfectly symmetrical geometry of the crossing seems inappropriate. An improvement through the specialization of different routes, that is, developing an asymmetric railhead profile crossing, is considered here to optimize the wheel-rail interaction.

To reduce maintenance costs of railway crossings, asymmetric solutions are already used. An example is the flange bearing crossing which support the wheel tread without discontinuity in the through route, while in the diverging route the wheel is lifted and supported on its flange. These crossings are not used in Europe, and the transition on the diverging route is very complex [18,19]. However, if the main route of the railway line is the through one a significant increase in crossing life can be achieved [20]. For conventional tread bearing crossings, a maintenance solution capable of restoring the crossing railhead geometry with the so-called wheel-matched technology (WMT) was developed and tested by Bombardier Transportation [21]. After the welding repair of the worn wing rails and crossing nose, a specific grinding process using grinding stones can generate surfaces that match the wheel profiles. Relevant benefits of a noise reduction of approximately 17 dB and a reduction of 70% in the forces transmitted to the bogie have been reported. The authors also claimed that this technology is a potential alternative for crossing with a movable nose.

While it is not clear if the technology is applicable to both through and diverging routes with the same efficiency, the aim of the shape modification is to generate a conformal contact between the rail and wheel to provide better guidance of the wheel during the transfer between the wing rail and nose and to spread the contact patch area, thereby reducing the contact pressure. The concept is further developed in the present study to minimize the magnitude of wheel-rail impacts.

2 Methods

Wheel/rail contact detection can be performed using multibody software packages, which use numerical methods suitable for evaluating the number of contact points, their locations, and contact patch shape. In this study, the VI-Rail package was used based on the Kik-Piotrowski theory [22] to model the normal contact problem and the FASTSIM algorithm [23] to solve the tangential contact problem.

A review of three contact models, including the VI-Rail model, considering the peculiar conditions that can be found when approaching a turnout, such as conformal contact, contact in the presence of sharp edges, and impacts [24]. The simulation results showed general agreement between the different formulations. A conformal wheel-rail contact can be obtained by milling both a special rail and crossing. Although it is relatively easy to obtain crossings with sufficient stock to be machined, a standard 60E1 rail is not sufficient to accommodate all contact points during crossing negotiations because of the limited width of the railhead. Therefore, a specific rail must be rolled to obtain a larger milling head to be milled afterwards.

2.1 Plain track modelling

In this study, the S1002 wheel profile, which is the most common in Europe [25], was used as a tool. The wheel, special rail profile, and contact patches are shown in Figure 2. As expected, the conformal contact extended to the entire profile length.

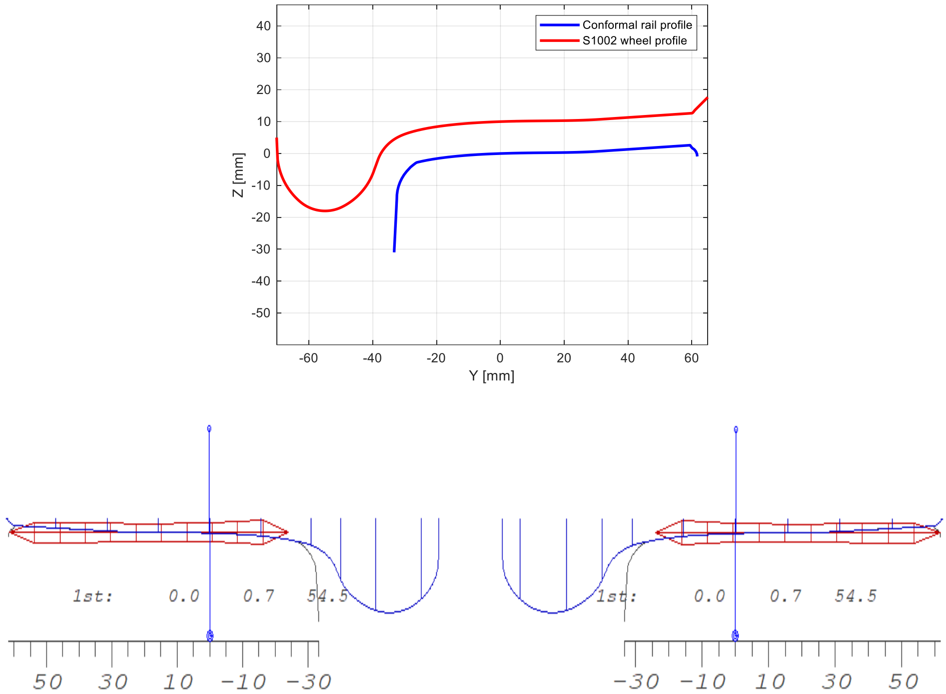

Figure 2: Top: S1002 wheel profile and the corresponding conformal profile (nominal track gauge and wheelset in the centred position) over a crossing or over a special rail. Bottom: Contact patches resulting from profiles coupling.

It should be noted that wheel and rail profiles typically tend to have greater conformity over time. The more conformal the contact is, the larger the changes in the rolling radius around the nominal position, and the equivalent conicity increases. This often occurs for worn wheel profiles and nominal rails, for which the *nonlinearity parameter* (NP) and *contact concentration index* (CCI) have been proposed to improve the wheel-rail contact evaluation in the case of high profile conformity [26]. Wheel-rail profile combinations with a greater conformity (i.e., with a small CCI) tend to wear less and become more stable over time.

Therefore, the proposed conformal crossing, in addition to its main scope, that is, the reduction of dynamic forces, can also benefit from optimized wheel/rail contact conditions.

2.2 Crossing modelling

A milling tool with an S1002 wheel profile was then used to simulate a milling process to generate a three-dimensional model of the possible crossing for a 60E1-170-0.12 RH (diverging to the right) turnout. It is not possible to obtain the same smoothness in the diverging route owing to the cutting of the conformal profile in the through direction. Therefore, the path encountered by a wheel running on the diverging route is affected by an important discontinuity after the crossing nose. The effect of a vehicle running at a maximum design speed of 30 km/h on the diverging route was investigated to analyse the actual contact conditions. This is an important task because high impact forces in the diverging route can modify the conformal profile in the through route owing to plastic deformation, partially eliminating the effect of the proposed modification.

Cross-sectional profiles at different longitudinal positions for both straight and diverging routes were extracted from the described 3D model to obtain a sufficiently narrowly spaced sequence of profiles. Figure 3 shows the profiles for the through route. These sequences were implemented in the multibody code to evaluate vehicle behaviour while passing over a crossing.

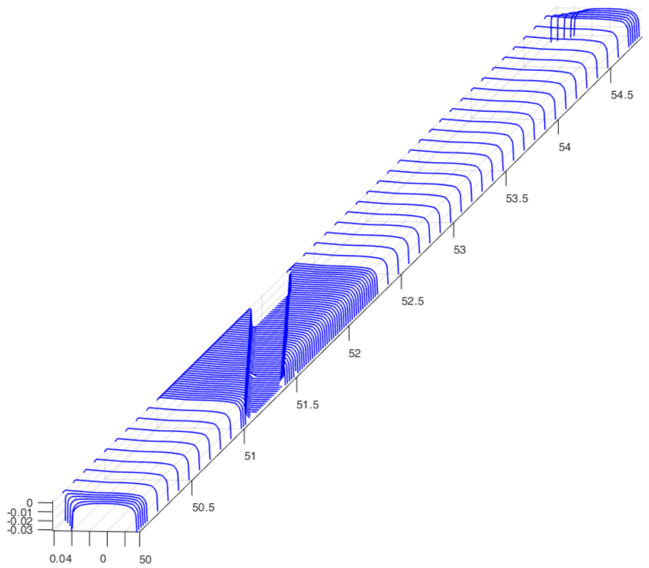

Figure 3: Sequence of profiles for the through route. Five sections are added at the beginning and at the end of the crossing (50 m and 55 m) to manage the transition between the 60E1 rail and the conformal rail.

Preliminary results showed that the wheel–rail contact in the diverging route generated a very high transient vertical, mainly because of the early load transfer from the wing rail to the crossing nose, requiring some efforts to mitigate this phenomenon. It should be emphasized that the scope of the research was not to optimize the path in the diverging route, but to keep vertical forces acceptable (like what happens in a conventional crossing) in this route. No optimization procedures were implemented, and a set of simulations was performed to obtain reasonably low contact forces with an easily machinable longitudinal profile in the diverging route.

A lift of 5.4 mm to all profiles with a 200 mm long linear transition ramp was eventually selected and applied to the wing rail. The “adjusted” crossing is shown in Figure 4. This modification does not affect the crossing nose geometry and the resulting interactions in a straight route, while simultaneously enhancing the wheel guidance during the passage over the crossing in the diverging route. Five rail sections were created to model the transitions between the standard 60E1 rail and the conformal profiles at the beginning and end of the crossing (50 and 55 m).

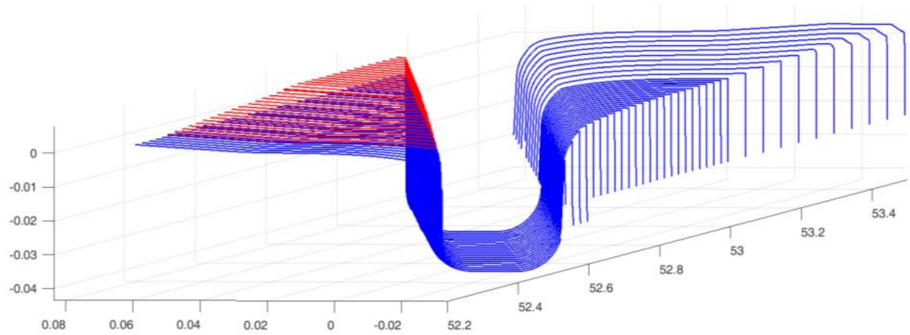

Figure 4: Modified (red) profiles to improve the wheel guidance from the wing rail to the crossing nose.

The crossing geometry was modelled on the right rail using variable profiles along the running direction, whereas the opposite stock rail was modelled on the left rail using a constant conformal profile. This simulates the introduction of a short piece of special conformal rail that supports the wheel along the entire crossing on the crossing panel. The track was modelled using a continuous support (the so-called *co-running model*) with constant mechanical properties (stiffness and damping parameters) according to benchmark specifications [9] to which the reader is referred for further details. A comparison of the behaviour of the co-running model with more complex models is given in [27] showing that the model is sufficiently accurate to predict the dynamics of the wheel-rail interaction.

3 Results

A model of the target of this research, that is, a 60E1-170-0.12 crossing, was not available as a three-dimensional model. The authors attempted to measure the profiles of an actual crossing; however, despite several attempts to smoothen and optimize the manually collected data, the results were still unsatisfactory [28].

The 56E1V-R245-1:9.25 crossing, whose three-dimensional geometry is available from the benchmark [9], was chosen as a reference for the present work. The differences between the 56E1V-R245-1:9.25 and 60E1-170-0.12 crossings are limited to the through route, and for the scope of the present research, it was assumed that the behaviour is the same.

3.1 Results running in through route

The first comparison between the reference crossing and conformal crossing was performed on a straight track, that is, by considering running over the crossing in the through direction at 100 km/h.

The reference crossing geometry and lateral displacement of the contact point along the through route are shown in Figure 5. Three main areas of discontinuity can be observed: i) at the entry leg of the crossing where the transition between the nominal rail profile and wing rail profile occurs, ii) where the contact point shifts from the wing rail to the crossing nose, and iii) at the crossing vee. This uneven wheel path generates extremely high vertical forces (DIF=5.9) that can rapidly damage the crossing geometry.

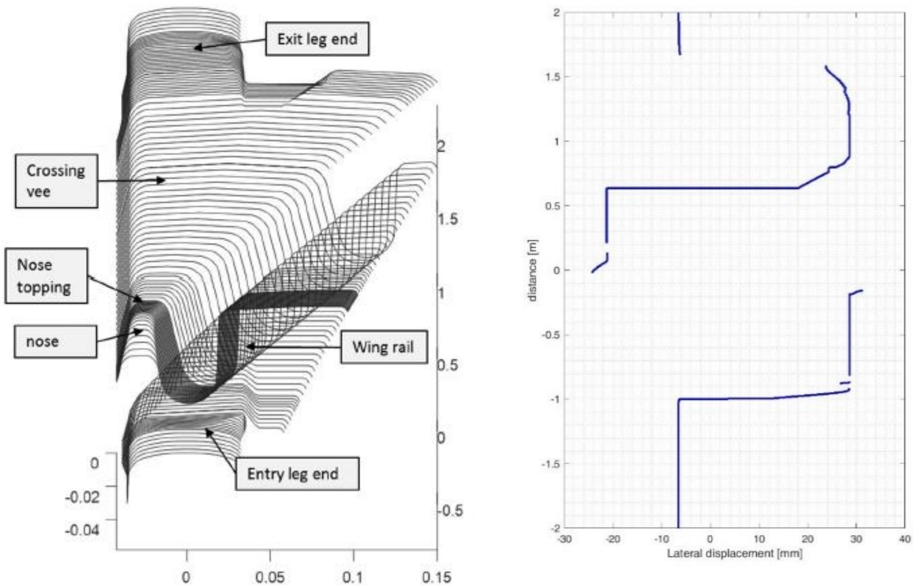

Figure 5: Profiles from three-dimensional model (left) and contact point position (right) over the reference crossing 56E1V-R245-1:9.25 (through direction) at 100 km/h.

This effect did not occur for the conformal crossing, in which a nearly perfect transition occurred between the wing rail and nose. The vertical forces from the reference and conformal crossings are compared in Figure 6, which shows a much greater regularity for the conformal crossing with a negligible increase from the static load (DIF=1.2). Moreover, for the conformal crossing, the largest vertical forces are generated outside the crossing area, that is, by the transition between the standard 60E1 rail profile and the conformal rail, as shown in Figure 6 (right) at distances of 50 m and 55 m. This confirms that the load transfer between the wing rail and nose is nearly perfect, and jumps are avoided, as shown by the vertical wheel displacement in Figure 7 and the sequence of the wheel/rail contact position shown in Figure 8.

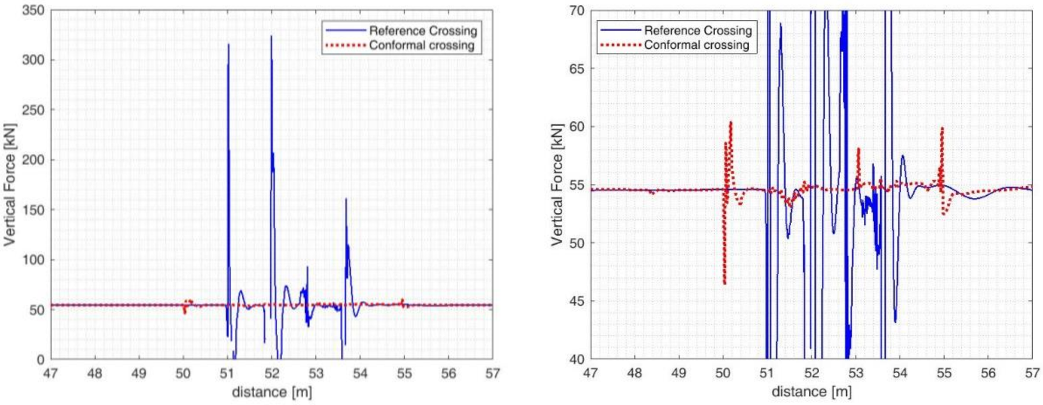

Figure 6: Results of the simulation passing at 100 km/h over the reference crossing and the conformal crossing. Vertical force in the full dynamic range (left) and in the 40÷70 kN range (right).

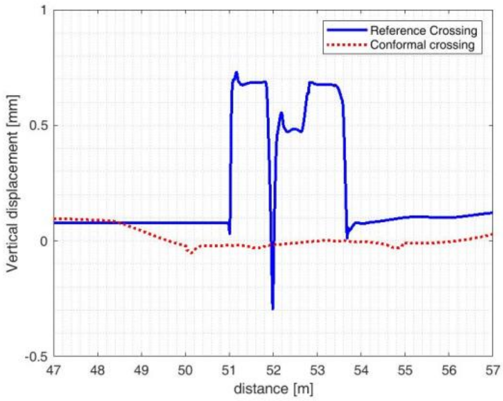

Figure 7: Vertical displacement of the wheel passing over the reference and the conformal crossing at 100 km/h.

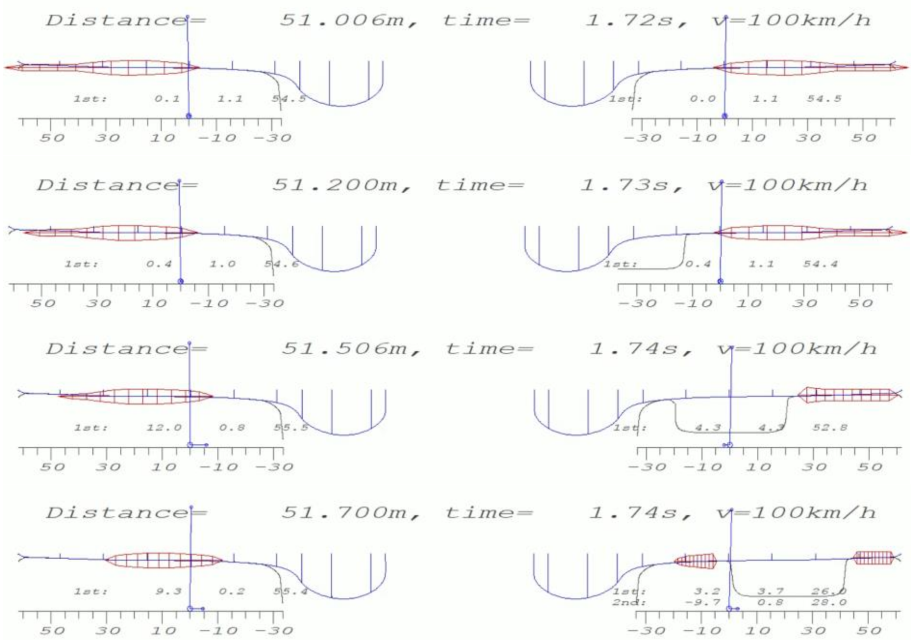

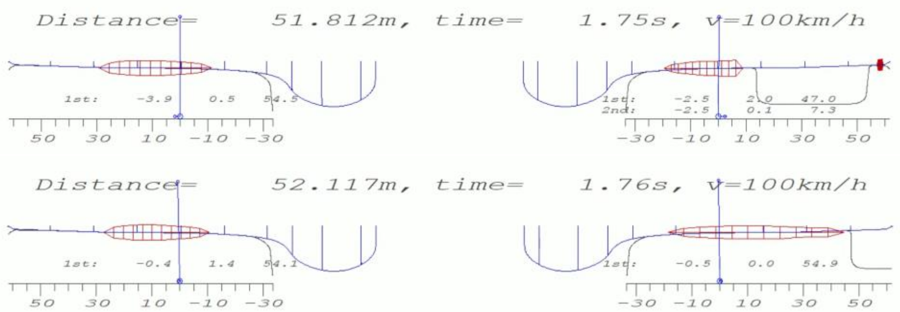

Figure 8: Sequence of the contacts along a crossing panel made of a conformal rail (left) and a conformal crossing (right) at 100 km/h. The effect of transition profiles from 60E1 rail to conformal rail are not shown.

3.2 Results in diverging route

To simulate the wheel–rail contact in the diverging route, the reference vehicle was run on a flat (non-canted) circular curve with the desired speed and curve radius to obtain the desired wheelsets and bogie attitude, including the lateral position of the front and rear wheelsets and the corresponding angles of attack. The crossing was then inserted on a straight track at the end of the curve where the vehicle behaviour was stationary. Therefore, the vehicle enters the crossing with the correct geometry and dynamic parameters.

The behaviour of the vehicle on both 56E1V-R245-1:9.25 and 60E1-170-0.12 straight crossings was simulated for both curve radii (170 and 245 m). The check rail was the same in all cases (i.e., one of the 56E1V-R245-1:9.25 turnouts), and the speed was set to 30 km/h. When wheelsets are grouped in a bogie, the behaviours of the leading and trailing wheelsets are completely different, as the latter tends to run more centered and with a lower angle of attack. As a result, the leading wheelset interacts with the check rail, which limits its lateral displacement, reaching a reasonably conformal contact on the crossing, whereas the trailing wheelset is more centered (Figure 9). As a result, it is impossible to obtain the same contact conditions for both wheelsets of a bogie. The lateral distances of the check rail and track gauge are parameters that can be investigated to minimize the resulting impact.

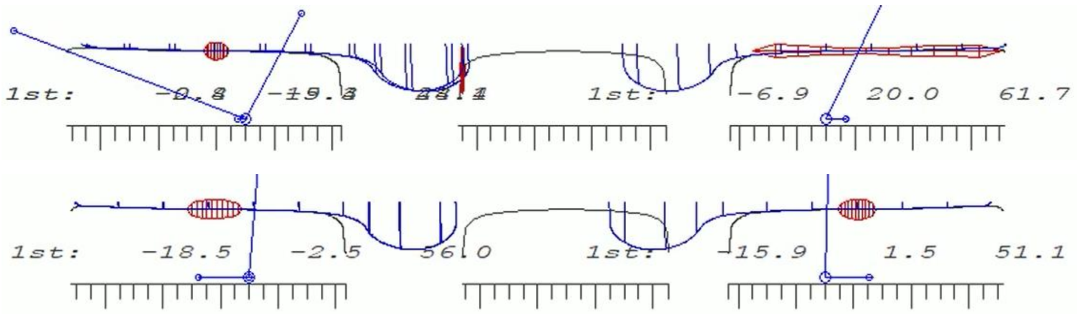

Figure 9: Leading (above) and trailing (below) wheelsets of the front bogie running over the diverging route of the conformal crossing. The difference in contact areas is evident.

The vertical forces for the wheel passing over the crossing showed a small dependency on the entering curve radius (170 m or 245 m). The vertical forces of the leading and trailing wheelsets for the 170 m curve (Figure 10) show that the reference crossing behaves better than the “adjusted” crossing in the diverging route with respect to the through route, exhibiting only one discontinuity at the entry leg. This may be due to either the lower speed (30 km/h instead of 100 km/h) or the initial lateral displacement of the leading wheelset running over the curve, which results in a smoother passage from the wing rail to the crossing nose.

Even if the signal is less smooth, the new crossing does not exhibit important discontinuities for the front wheel, while for the rear wheel, a short loss of contact can be seen during the passage over the “adjusted” crossing nose. This is believed not to be a major drawback of the geometry of the crossing, as the scope of the research was focused on turnouts that are rarely operated in the diverging route.

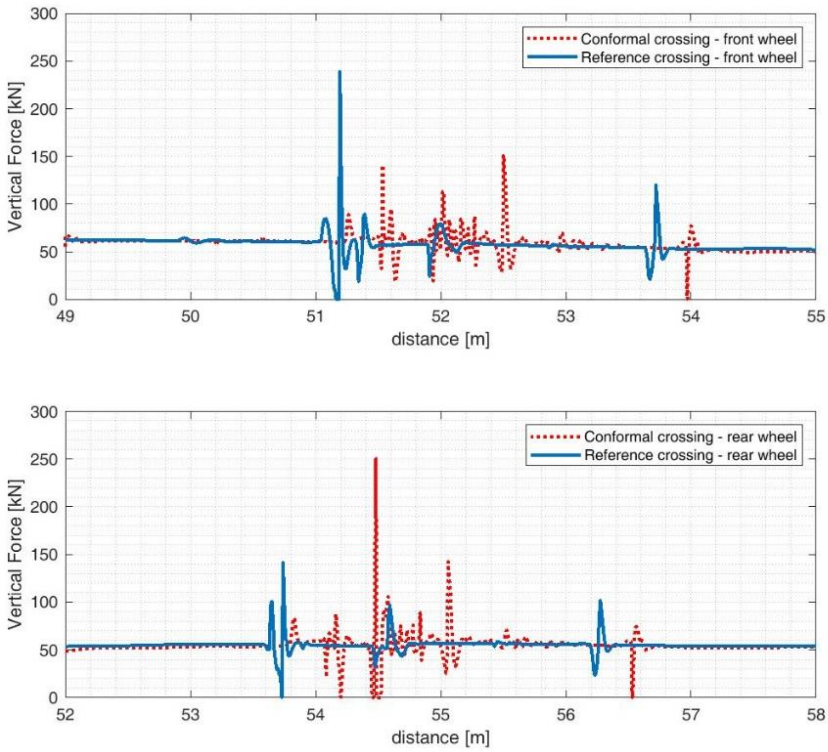

Figure 10: Vertical force of the leading (top) and the trailing (bottom) wheels passing over the “adjusted” crossing (dashed line) and the reference crossing (solid line) in a curve of 170 m.

4 Conclusions and Contributions

Although optimization processes regarding wing rail and nose shapes and crossing supporting stiffness (rail pads and under sleeper pads) have been proposed by several authors, dip angle irregularity between the wing rail and nose cannot be avoided by standard geometries, especially if large crossing angles are considered.

The high vertical loads generated by a wheel running over a common crossing can only be mitigated. This study approaches the problem by considering the design of the crossing panel components (straight main rail and common crossing) using the concept of conformal wheel-rail profiles to create a continuous and seamless wheel support during travel on the crossing.

A conformal crossing with asymmetric profiles based on the complementary S1002 wheel profile was designed and implemented in a multibody code to simulate the dynamic behaviour of a vehicle running at 100 km/h on the through route. The proposed crossing is particularly suited for mainline low-radius turnouts that are rarely operated at a speed on the order of 30 km/h in the diverging route.

The conformal crossing was successful, as it featured nearly perfect support of the wheel over the crossing in the through route, completely avoiding wheel jumps and impact forces. The modified geometry affects the contacts in the diverging route because the angles of attack of the wheelsets of a bogie in small radius curves are different, and a unique, optimized solution does not exist. An empirical and particularly simple crossing shape modification was found to generate acceptably smooth running in the diverging route, limiting the impacts to a reasonably low value.

References

[1] G. Megna, A. Bracciali, N. K. Mandal, “Design, wheel-rail interaction and testing of an innovative reinforced smooth transition insulated rail joint”, Wear, vol. 530–531, p. 205038, 2023, doi: 10.1016/j.wear.2023.205038.

[2] R. F. Lagos, A. Alonso, J. Vinolas, and X. Pérez, “Rail vehicle passing through a turnout: analysis of different turnout designs and wheel profiles”, Proceedings of the Institution of Mechanical Engineers, Part F: Journal of Rail and Rapid Transit, vol. 226, no. 6, pp. 587–602, 2012, doi: 10.1177/0954409712445114.

[3] B. A. Pålsson, “A linear wheel–crossing interaction model”, Proceedings of the Institution of Mechanical Engineers, Part F: Journal of Rail and Rapid Transit, vol. 232, no. 10, pp. 2431–2443, 2018, doi: 10.1177/0954409718772984.

[4] P. T. Torstensson, G. Squicciarini, M. Krüger, B. A. Pålsson, J. C. O. Nielsen, D. J. Thompson, “Wheel–rail impact loads and noise generated at railway crossings – Influence of vehicle speed and crossing dip angle”, Journal of Sound and Vibration, vol. 456, pp. 119–136, 2019, doi: 10.1016/j.jsv.2019.04.034.

[5] R. Skrypnyk, B. A. Pålsson, J. C. O. Nielsen, M. Ekh, “On the influence of crossing angle on long-term rail damage evolution in railway crossings”, International Journal of Rail Transportation, vol. 9, no. 6, pp. 503–519, 2021, doi: 10.1080/23248378.2020.1864794.

[6] EN 13232-6:2005+A1:2011 Railway applications - Track - Switches and crossings - Part 6: Fixed common and obtuse crossings, n.d.

[7] M. D. G. Milosevic, B. A. Pålsson, A. Nissen, J. C. O. Nielsen, H. Johansson, “Condition Monitoring of Railway Crossing Geometry via Measured and Simulated Track Responses”, Sensors, vol. 22, no. 3, Art. no. 3, 2022, doi: 10.3390/s22031012.

[8] H. H. Jenkins, J. E. Stephenson, G. A. Clayton, G. W. Morland, D. Lyon, “The effect of track and vehicle parameters on wheel/rail vertical dynamic forces”, Railway Engineering Journal, vol. 3, no. 1, 1974,
[9] Y. Bezin, B. A. Pålsson, “Multibody simulation benchmark for dynamic vehicle-track interaction in switches and crossings: modelling description and simulation tasks”, Vehicle System Dynamics, vol. 61, no. 3, pp. 644–659, 2023, doi: 10.1080/00423114.2021.1942079.
[10] Y. Bezin et al., “Multibody simulation benchmark for dynamic vehicle–track interaction in switches and crossings: results and method statements”, Vehicle System Dynamics, vol. 61, no. 3, pp. 660–697, 2023, doi: 10.1080/00423114.2021.1959038.
[11] N. Bosso, A. Bracciali, G. Megna, N. Zampieri, “Effects of geometric track irregularities on vehicle dynamic behaviour when running through a turnout”, Vehicle System Dynamics, pp. 1–17, 2021, doi: 10.1080/00423114.2021.1957127.
[12] C. Wan, V. L. Markine, and I. Y. Shevtsov, “Improvement of train-track interaction in turnouts by optimising the shape of crossing nose”.
[13] B. A. Pålsson, “Optimisation of railway crossing geometry considering a representative set of wheel profiles”, Vehicle System Dynamics, vol. 53, no. 2, pp. 274–301, 2015, doi: 10.1080/00423114.2014.998242.
[14] C. Wan, V. Markine, I. Shevtsov, “Optimisation of the elastic track properties of turnout crossings”, Proceedings of the Institution of Mechanical Engineers, Part F: Journal of Rail and Rapid Transit, vol. 230, no. 2, pp. 360–373, 2016, doi: 10.1177/0954409714542478.
[15] D. Nicklisch, E. Kassa, J. Nielsen, M. Ekh, and S. Iwnicki, “Geometry and stiffness optimization for switches and crossings, and simulation of material degradation”, Proceedings of the Institution of Mechanical Engineers, Part F: Journal of Rail and Rapid Transit, vol. 224, no. 4, pp. 279–292, 2010, doi: 10.1243/09544097JRRT348.
[16] I. Grossoni, Y. Bezin, S. Neves, “Optimisation of support stiffness at railway crossings”, Vehicle System Dynamics, vol. 56, no. 7, pp. 1072–1096, 2018, doi: 10.1080/00423114.2017.1404617.
[17] Y. Bezin, D. Kostovasilis, and B. Sambo, “Reducing Impact Loads at Railway Crossings Using Tuned Resilient Elements” in “Advances in Dynamics of Vehicles on Roads and Tracks”, M. Klomp, F. Bruzelius, J. Nielsen, and A. Hillemyr, (Editors), Lecture Notes in Mechanical Engineering, Cham: Springer International Publishing, pp. 390–396, 2020, doi: 10.1007/978-3-030-38077-9_46.
[18] Y. Gao, J. Xu, P. Wang, Z. Dong, Y. Liu, K. Wang, “Numerical study of the transition characteristics and related degradation at the flange bearing frog”, Proceedings of the Institution of Mechanical Engineers, Part F: Journal of Rail and Rapid Transit, vol. 235, no. 1, pp. 94–106, 2021, doi: 10.1177/0954409720906636.
[19] J. Xu, Y. Gao, P. Wang, B. An, J. Chen, R. Chen, “Numerical analysis for investigating wheel-rail impact contact in a flange bearing frog crossing”, Wear, vol. 450–451, p. 203253, 2020, doi: 10.1016/j.wear.2020.203253.

[20] C. T. Rapp, R. G. Kernes, M. R. Saat, “Overview of issues and research related to special trackwork for shared high-speed-rail passenger and heavy-axle-load freight operations”, Proceedings of the Institution of Mechanical Engineers, Part F: Journal of Rail and Rapid Transit, vol. 228, no. 5, pp. 557–565, 2014, doi: 10.1177/0954409713486260.
[21] H. Skoblenick, P. Eng, B. Transportation, K. On, “Wheel Matched Technology (WMT) for Railway Crossings”.
[22] J. Piotrowski, W. Kik, “A simplified model of wheel/rail contact mechanics for non-Hertzian problems and its application in rail vehicle dynamic simulations”, Vehicle System Dynamics, vol. 46, no. 1–2, pp. 27–48, 2008, doi: 10.1080/00423110701586444.
[23] J. J. Kalker, “A Fast Algorithm for the Simplified Theory of Rolling Contact”, Vehicle System Dynamics, vol. 11, no. 1, pp. 1–13, 1982, doi: 10.1080/00423118208968684.
[24] H. Magalhaes et al., “Wheel-rail contact models in the presence of switches and crossings”, Vehicle System Dynamics, vol. 61, no. 3, pp. 838–870, 2023, doi: 10.1080/00423114.2022.2045026.
[25] EN 13715:2020 Railway applications - Wheelsets and bogies - Wheels - Tread profile.
[26] O. Polach, D. Nicklisch, “Wheel/rail contact geometry parameters in regard to vehicle behaviour and their alteration with wear”, Wear, vol. 366–367, pp. 200–208, 2016, doi: 10.1016/j.wear.2016.03.029.
[27] B. A. Pålsson et al., “A comparison of track model formulations for simulation of dynamic vehicle–track interaction in switches and crossings”, Vehicle System Dynamics, vol. 61, no. 3, pp. 698–724, 2023, doi: 10.1080/00423114.2021.1983183.
[28] Y. Bezin, B. Sambo, H. Magalhaes, W. Kik, G. Megna, J. N. Costa, “Challenges and methodology for pre-processing measured and new rail profiles to efficiently simulate wheel-rail interaction in switches and crossings”, Vehicle System Dynamics, vol. 61, no. 3, pp. 799–820, 2023, doi: 10.1080/00423114.2021.2014897.